

Supplementary Material

Supplementary Table 1 Legend	2
Supplementary Table 2	3
Supplementary Table 3	4
Supplementary Table 4 Legend	5
Supplementary Table 5	6
Supplementary Figure Legends	7
Supplementary Video Legend	12
Supplementary Figures	13

Supplementary Table 1. A list of copy number alterations, rearrangements and short variants detected by Foundation Medicine NGS analysis in the 12 cases with archival tissue and/or pre-treatment and post-progression biopsies.

Supplementary Table 2. Confirmation of cis configuration of *BRCA1* primary and secondary mutations in case 4 by colony PCR.

Mutation	N colonies
c.2042_2043insT	11
Cis: c.2042_2043insT and c.1835_1964del130	7
Trans: c.2042_2043insT and c.1835_1964del130	0
Wild-type	3

Supplementary Table 3. IC₅₀ (μM) values of the PARPi and platinum drugs in parental OVCAR8 cell line and OVCAR8 *RAD51C* KO clone, and the fold change in IC₅₀ values.

	<i>IC₅₀</i> (μM)		<i>Fold change</i>
	Parental OVCAR8	<i>RAD51C</i> KO	
<i>Rucaparib</i>	4.556	0.019	237
<i>Niraparib</i>	0.821	0.023	35
<i>Olaparib</i>	4.715	0.038	123.7
<i>Talazoparib</i>	0.038	0.0003	126.7
<i>Veliparib</i>	>20	0.612	NC
<i>Carboplatin</i>	11.57	0.228	50.7
<i>Cisplatin</i>	2.56	0.085	92.9

Supplementary Table 4. Copy number estimation by SNP array in the archival tumor tissue of the patient identified to have a germline *RAD51C* mutation (c.577C>T). Three copies of the *RAD51C* gene were observed.

Supplementary Table 5. Sequences of primers used for site-directed mutagenesis.

<i>Primer</i>	<i>Sequence</i>
RAD51C_R193WFWD	5'caagggagaggaacactggaaagcttggagg3'
RAD51C_R193WREV	5'cctccaaagcttccagtgttcctccttg3'
RAD51C_R193RFWD	5'caagggagaggaacacagaaaagcttggagg3'
RAD51C_R193RREV	5'cctccaaagcttttctgttcctccttg3'
RAD51C_R193LFWD	5'caagggagaggaacactaaaagcttggagg3'
RAD51C_R193LREV	5'cctccaaagctttaagtgttcctccttg3'
RAD51C_H192GFWD	5'cacaagggagaggaaggccgaaaagcttgg3'
RAD51C_H192GREV	5'ccaaagctttcggccttcctccttg3'
RAD51C_R193GFWD	5'caagggagaggaaggcggaaaagcttggagg3'
RAD51C_R193GREV	5'cctccaaagctttccgccttcctccttg3'
RAD51C_R193XFWD	5'caagggagaggaacactgaaaagcttggagg3'
RAD51C_R193XREV	5'cctccaaagctttcagtgttcctccttg3'

Supplementary Figure Legends

Supplementary Figure 1. Foundation Medicine NGS analysis of the 12 cases with archival tissue and/or pre-treatment and post-progression biopsies. Of the 289 cancer-related changes assessed by the Foundation Medicine NGS assay, copy number alterations, rearrangements or short variants were identified in 41 genes. Corresponding mutations in *TP53* gene were detected in all 12 cases in each of the tested specimens (archival, pre-treatment, and post-progression). In case 2 with *BRCA1* mutation (c.5346G>A) but without secondary mutation identified in the post-progression biopsy, no other alterations were identified that could explain resistance to rucaparib.

Supplementary Figure 2. Sanger sequencing trace of the primary and secondary *BRCA1* mutations in cis configuration in case 4 post-progression biopsy sample.

Supplementary Figure 3. *In vitro* response to PARP inhibitor therapy and platinum agents in *RAD51C* deficient cell lines, with primary or secondary mutations in *RAD51C*. a-f, *In vitro* response to platinum agents (cisplatin and carboplatin) and to PARP inhibitors (niraparib, olaparib, talazoparib and veliparib) in Parental OVCAR8 cell line, OVCAR8 *RAD51C* KO clone and OVCAR8 *RAD51C* KO clone transduced with WT, primary or secondary mutant *RAD51C* transcripts after treatment for 6 days. g, Western Blotting of RAD51C and Tubulin (control) protein expression in parental OVCAR8 cell line and OVCAR8 *RAD51C* KO. n \geq 3 experiments. h, Western Blotting of RAD51C and GAPDH (control) protein expression in parental OVCAR8 cell line, OVCAR8 *RAD51C* KO clone and OVCAR8 *RAD51C* KO clone transduced with WT, primary or secondary mutant *RAD51C* transcripts i, Western Blotting quantification of RAD51C and GAPDH (control) protein expression.

Supplementary Figure 4. RAD51 foci formation in geminin positive cells deficient for *RAD51C*, complemented with primary or secondary mutations in *RAD51C*. a-e, Quantification of RAD51

foci formation in geminin positive cells. OVCAR8 *RAD51C* KO cells were transfected with plasmids expressing the wild-type *RAD51C* gene with the PAM site deleted (PAM), the primary *RAD51C* nonsense mutation (R193*), the secondary *RAD51C* reversion mutation (R193W), or the secondary *RAD51C* reversion mutation (H192_R193GG). The response of these cells to ionizing radiation (10 Gy) or to 10 μ M Rucaparib was compared at the time-points shown to wild-type (parental) or untransfected knockout (KO) cells. n=8 (4 fields of view from 2 independent experiments) for each cell type and treatment. Mean \pm SEM.

Supplementary Figure 5. Diagram of HR reporter assay. The DR-GFP reporter consists of two disrupted GFP genes. A double-stranded break (DSB) introduced by I-SceI endonuclease in SceGFP can be repaired by HR using iGFP to restore a functional GFP+ gene.

Supplementary Figure 6. RAD51C expression in MCF10A cells and in yeast. *RAD51C* expression was examined in the MCF10A DR-GFP cells and in yeast cells used for Y2H analysis. Ectopic expression of each secondary mutation demonstrates full-length *RAD51C* expression, unlike *RAD51C* R193*. **a**, Nuclear extracts of MCF10A cells expressing the indicated *RAD51C* mutant were tested for *RAD51C* protein levels by Western blotting. PCNA expression was used as a nuclear loading control. *indicates a nonspecific band. **b**, Protein samples were extracted from yeast expressing pGAD-XRCC3 and the indicated pGBD-*RAD51C* construct. *indicates a nonspecific band.

Supplementary Figure 7. Analysis of serial sections by direct PCR sequencing approach of a post-progression biopsy containing multiple secondary mutations in *RAD51C*. **a**, H&E staining of the serial sections of the post-progression biopsy (*RAD51C* case). **b**, Detected mutational frequencies in the serial sections of the post-progression biopsy.

Supplementary Figure 8. Molecular Dynamics Modeling of WT RAD51D protein and RAD51D protein with secondary mutation c.770_776delinsA, p.S257_R259delinsK.

a-b, Molecular dynamics modeling of WT RAD51D. Six monomers of WT RAD51D (alternating blue and grey, helix-sheet-loop representation) were modelled in a filament configuration with dsDNA (salmon and pink, ball and stick representation). **a**, The Ser257-Gly258-Arg259 motif that is deleted in the secondary mutation interacts with the dsDNA strand. The primary mutation is a frame shift from this residue resulting in 50aa of altered sequence and a premature stop codon. Sequence departure from the crystal structure precluded accurate modeling of the primary mutation; however, from the WT modeling it is inferred to abolish dsDNA interaction. **b**, Detail of the interaction between residues 257-259 and the dsDNA with three RAD51D monomers visible (orange, grey and brown in helix-sheet-loop representation and the deletion residues highlighted in ball and stick representation) shows the wild-type Arg259 interacting with the DNA through the positively charged nitrogen atoms (blue), and a weaker interaction between the hydroxyl group of Ser257 (red). **c**, In the secondary mutant with deletion of Ser257-Gly258 and substitution of lysine at Arg259 the shortening of the loop does not appear to sterically hinder interaction with the dsDNA and the charge based interaction is maintained by the positively charged nitrogen atom of the lysine (blue). **d**, Phylogenetic alignment of mammalian RAD51D regions homologous to the Ser257-Arg259 deletion. Eleven of 34 mammals have substitutions of lysine for arginine at the position homologous to human Arg259, indicating that this is an evolutionarily tolerated substitution and unlikely to present a major phenotypic effect. Human *Homo sapiens* ENSP00000466399; Gorilla *Gorilla gorilla* ENSGGOP00000000358; Chimp *Pan troglodytes* ENSPTRP00000046398; Orangutan *Pongo abelii* ENSPPYP00000009193; Gibbon *Nomascus leucogenys* ENSNLEP00000002225; Vervet *Chlorocebus sabaues* ENSCSAP00000002609; Olive baboon *Papio anubis* ENSPANP00000020033; Marmoset *Callithrix jacchus* ENSCJAP00000027151; Tarsier *Tarsius syrichta* ENSTSYYP00000002243; Bushbaby *Otolemur garnettii* ENSOGAP00000008835; Mouse *Mus musculus* ENSMUSP00000018985; Rat *Rattus norvegicus* ENSRNOP000000036257; Chinese Hamster *Cricetulus griseus* XP_003495849.1;

Squirrel *Ictidomys tridecemlineatus* ENSSTOP00000022353; Guinea Pig *Cavia porcellus* ENSCPOP00000017272; Pika *Ochotona princeps* ENSOPRP00000010741; Sheep *Ovis aries* ENSOARP00000008076; Cow *Bos taurus* ENSBTAP00000025404; Pig *Sus scrofa* ENSSSCP00000027415; Dolphin *Tursiops truncatus* ENSTTRP00000014683; Dog *Canis familiaris* ENSCAFP00000027051; Panda *Ailuropoda melanoleuca* ENSAMEP00000015383; Cat *Felis catus* ENSFCAP00000023805; Horse *Equus caballus* ENSECAP00000012028; Microbat *Myotis lucifugus* ENSMLUP00000011374; Megabat *Pteropus vampyrus* ENSPVAP00000003694; Shrew *Sorex araneus* ENSSARP00000000796; Hedgehog *Erinaceus europaeus* ENSEEUP00000001339; Tenrec *Echinops telfairi* ENSETEP00000009798; Hyrax *Procavia capensis* ENSPCAP00000006649; Elephant *Loxodonta africana* ENSLAFP00000015357; Armadillo *Dasypus novemcinctus* ENSDNOP000000031581; Opossum *Monodelphis domestica* ENSMODP000000023889; TasmanianDevil *Sarcophilus harrisii* ENSSHAP00000005158.

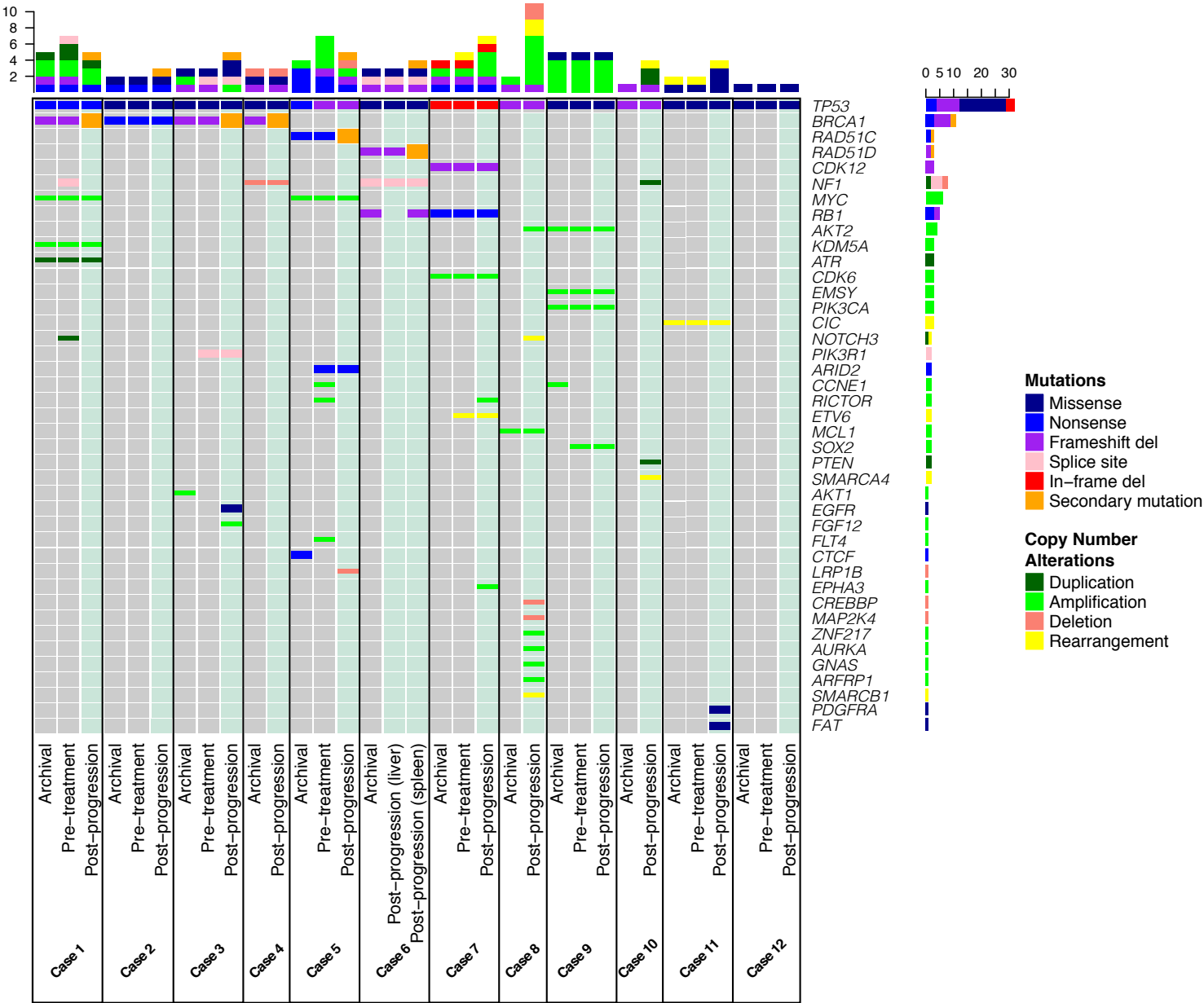
Supplementary Figure 9. *In vitro* response to PARP inhibitor therapy and cisplatin in *RAD51D* deficient CHO cell line, with primary or secondary mutation in *RAD51D*. a-e, *In vitro* response to cisplatin and to PARP inhibitors (niraparib, olaparib, talazoparib and veliparib) in parental CHO cell line, *RAD51D* KO clone and *RAD51D* KO clone transduced with WT, primary or secondary mutant *RAD51D* transcripts after treatment for 6 days. f, Western Blotting of *RAD51D* N-terminal, C-terminal and Tubulin (control) protein expression in parental CHO cell line, *RAD51D* KO clone and *RAD51D* KO clone transduced with WT, primary or secondary mutant *RAD51D* transcripts.

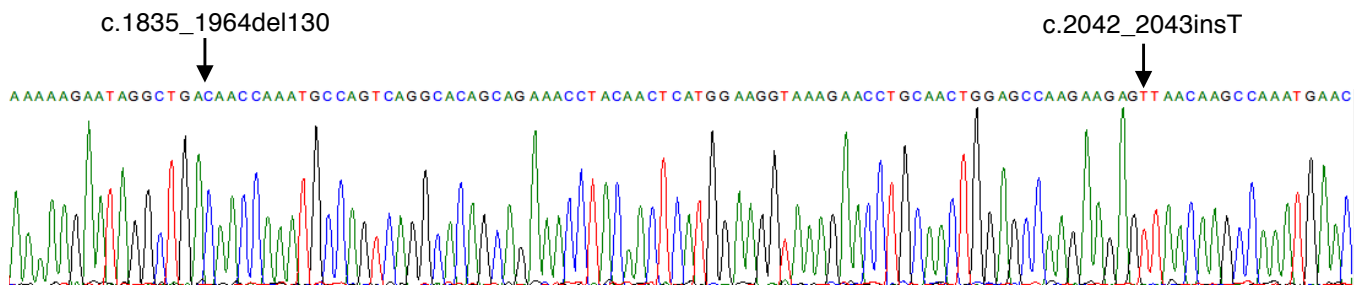
Supplementary Figure 10. Examination of the parental PEO4 cell line, PEO4 cells with the homozygous frameshift *RAD51D* mutation (c.762_763del, D254E*fs72) in the same exon as the primary mutation and PEO4 cells with the homozygous secondary *RAD51D* mutation (c.770_776delinsA, S257_R259delinsK) using: a, Cell viability assay after treatment with cisplatin

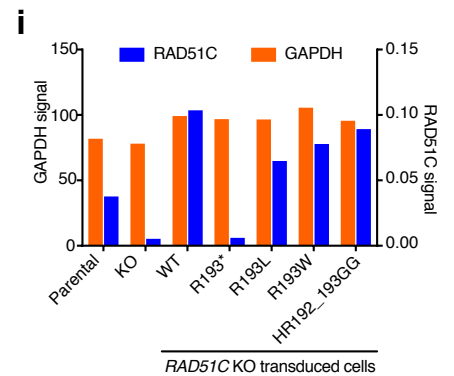
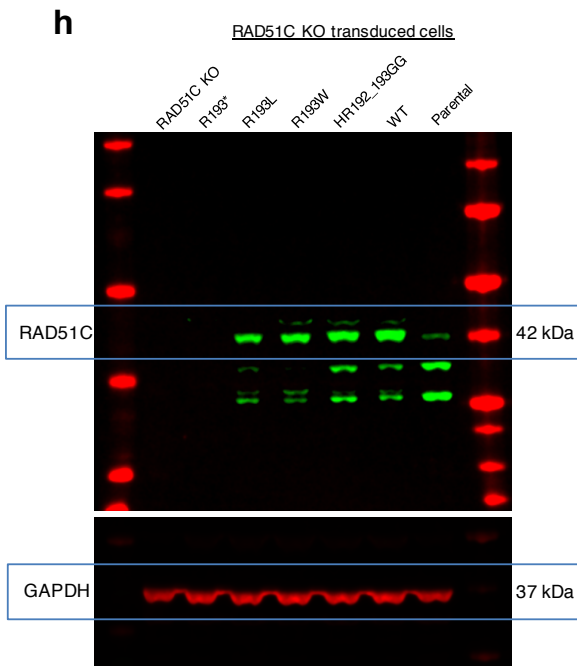
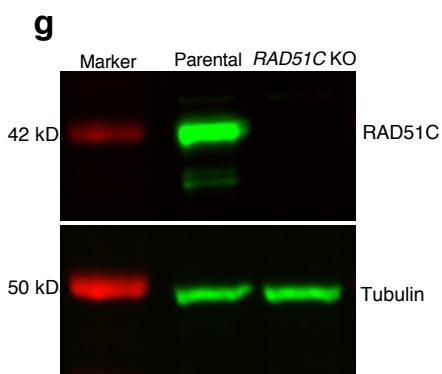
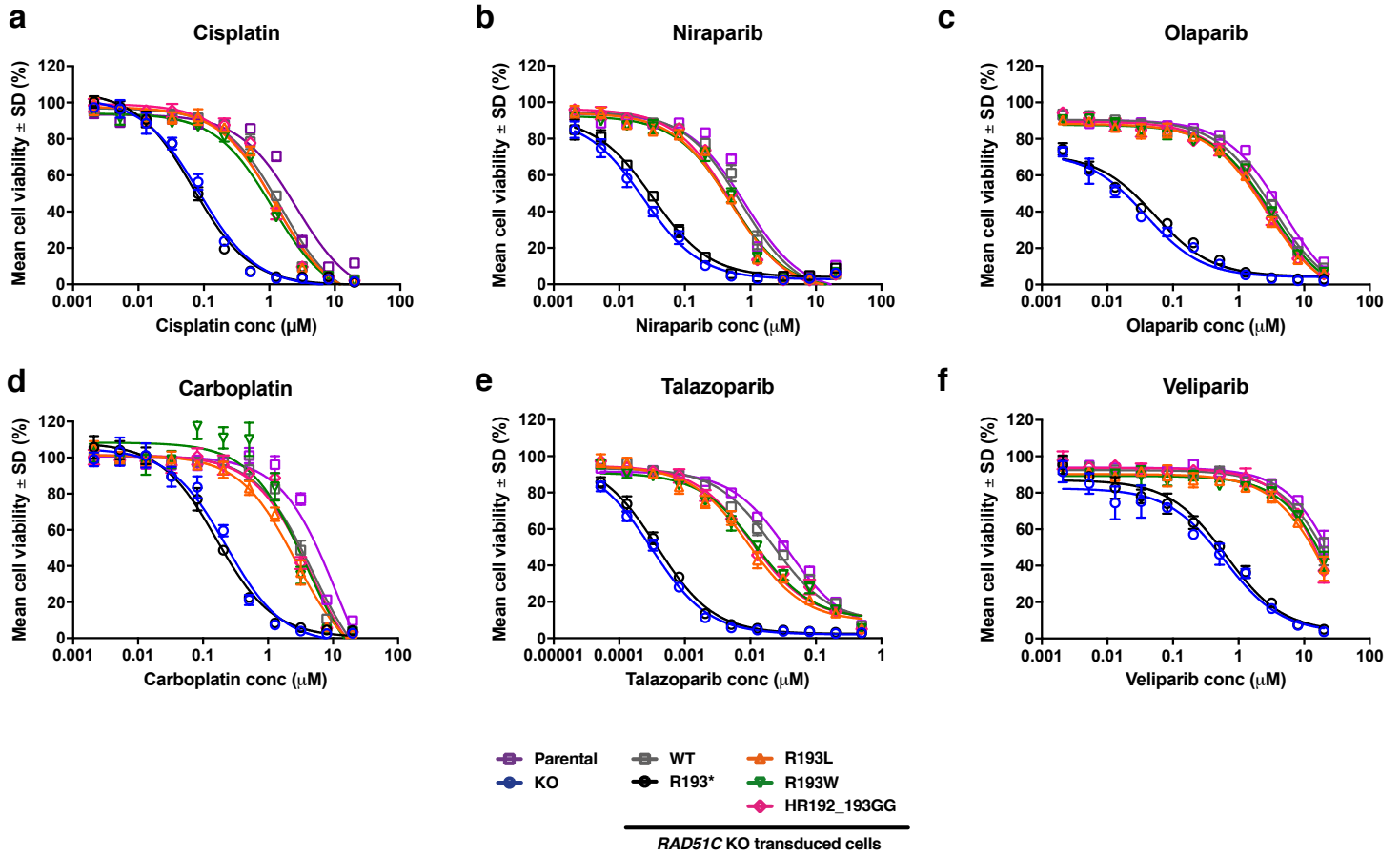
for 7 days. **b**, Western Blotting of RAD51D N-terminal, C-terminal and B-Actin (control) protein expression.

Supplementary Figure 11. Modeling of tumor clonal fractions in the post-progression biopsy sample with germline *RAD51C* mutation and multiple secondary mutations. Allele frequencies of the germline and secondary mutations determined by Foundation Medicine NGS. Based on the detected allele frequencies as well as copy number model and estimated tumor content, the tumor clonal fractions containing the different mutations were inferred. Within the tissue specimen, tumor cells (predicted to be triploid) are estimated to encompass 62% of cells, and normal cells (predicted to be diploid) are estimated to encompass the remaining 38% of cells.

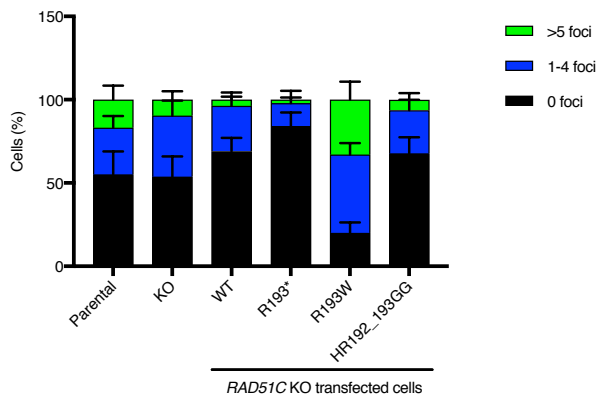
Supplementary Video. Molecular Dynamics Modeling of WT RAD51D monofilament interaction with dsDNA. Molecular dynamics modelling of a 6 monomer helical filament complex of wild-type RAD51D with dsDNA. Monomers of RAD51D are represented as alternating blue and grey space filling representation. At 8s into the video the representation zooms in to the Ser257-Gly258-Arg259 region and the interaction of these residues with dsDNA. These residues are highlighted in red space filling representation, which transitions to a stick representation showing the positively charged nitrogen atoms (blue) of the Arg 259 interacting with the dsDNA.



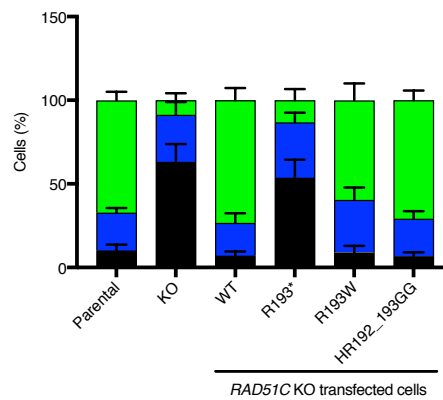




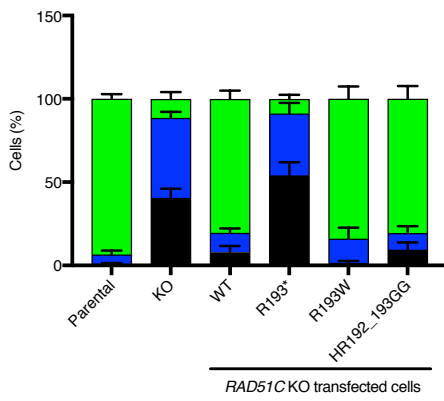
a Untreated



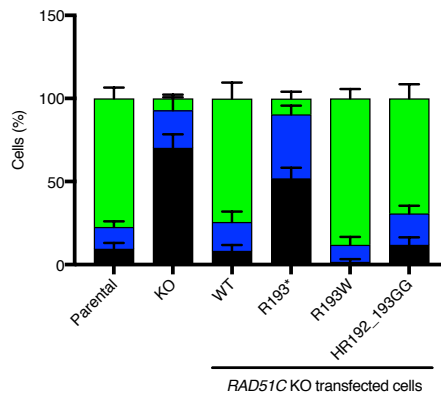
b Ionizing radiation



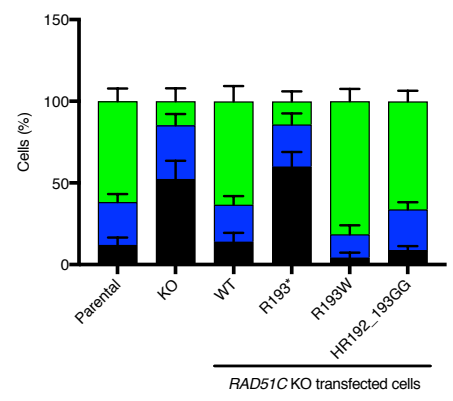
c 24 hr rucaparib 10 μ M

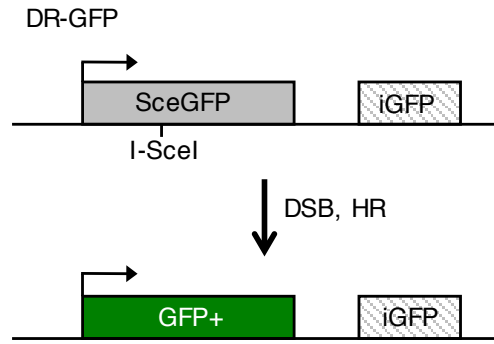


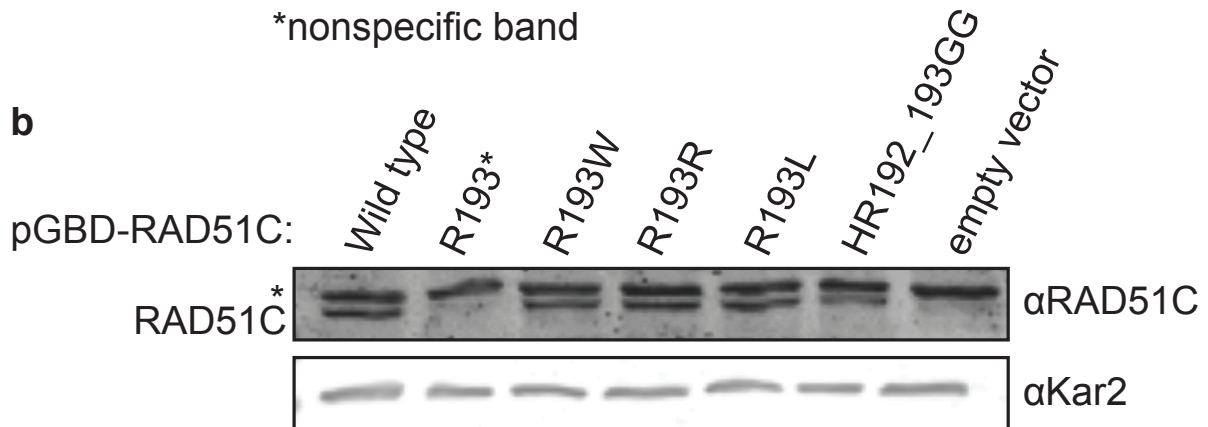
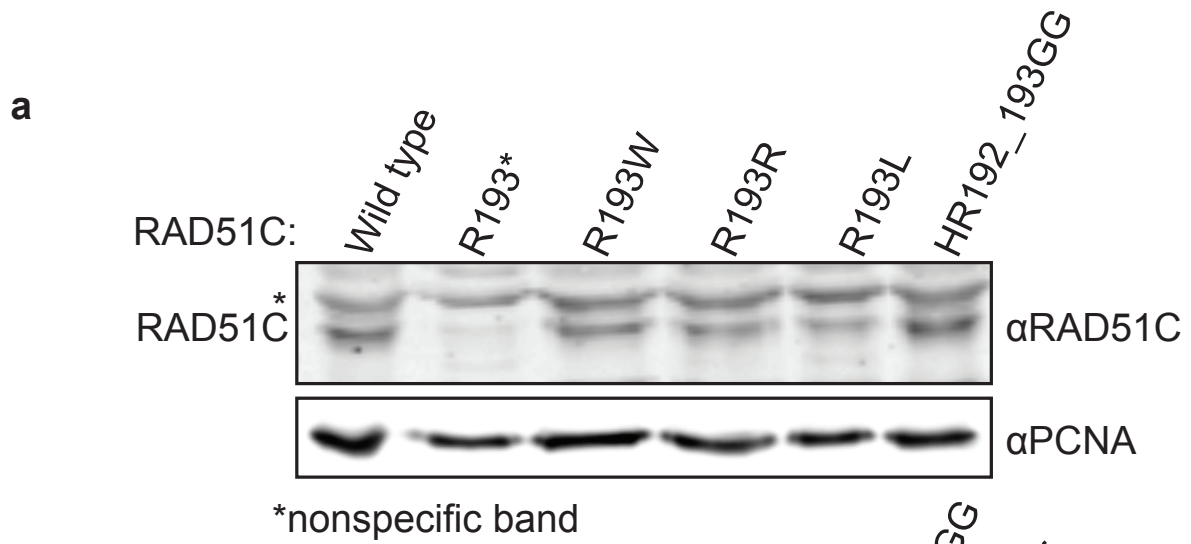
d 48 hr rucaparib 10 μ M



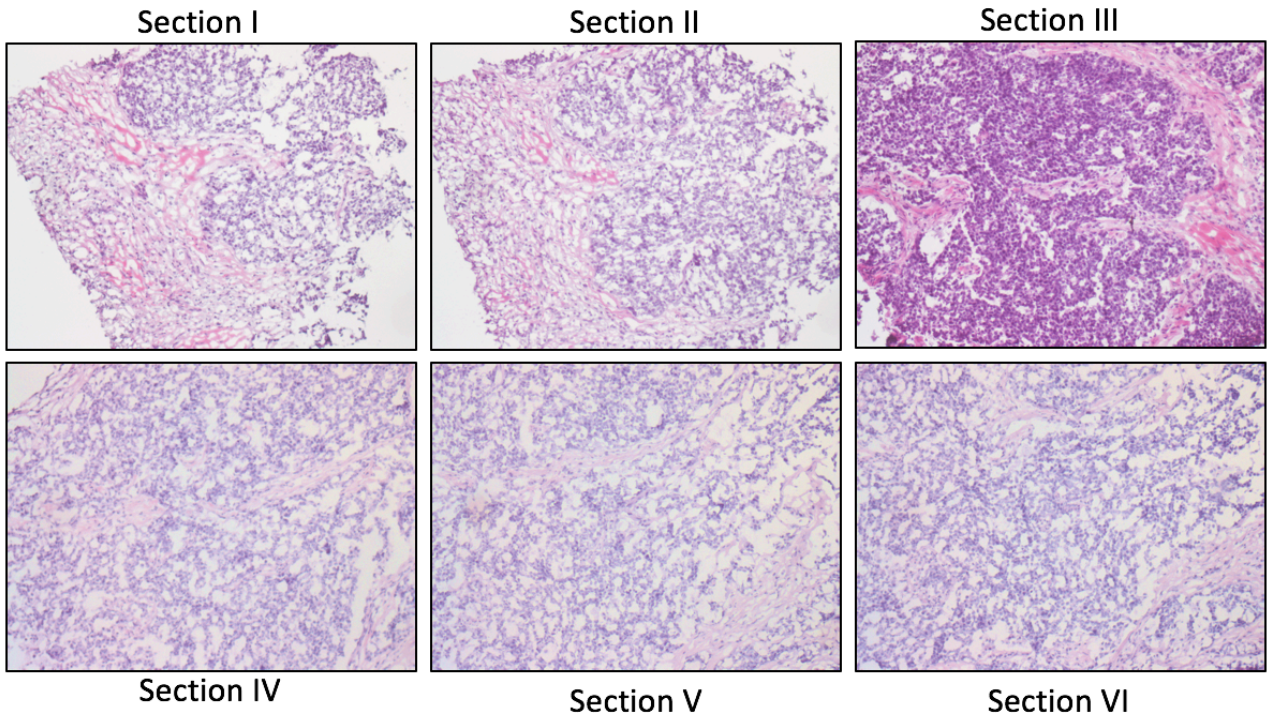
e 72 hr rucaparib 10 μ M



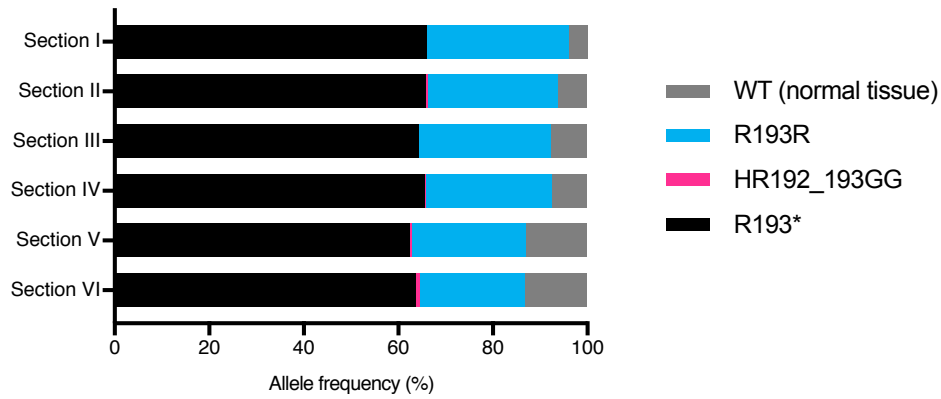




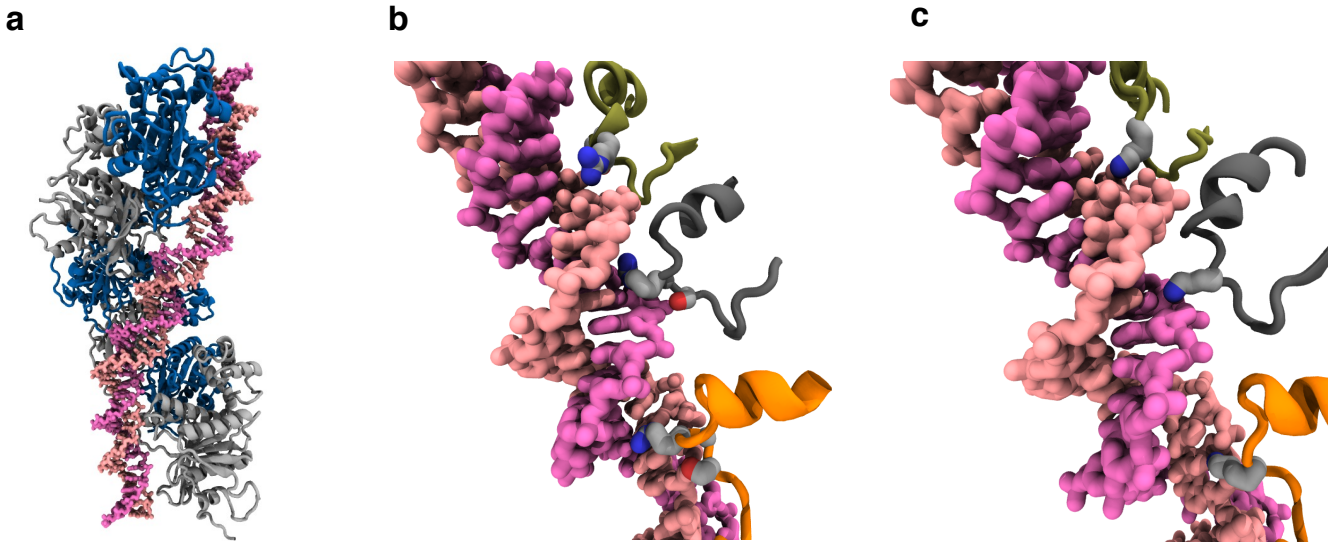
a



b

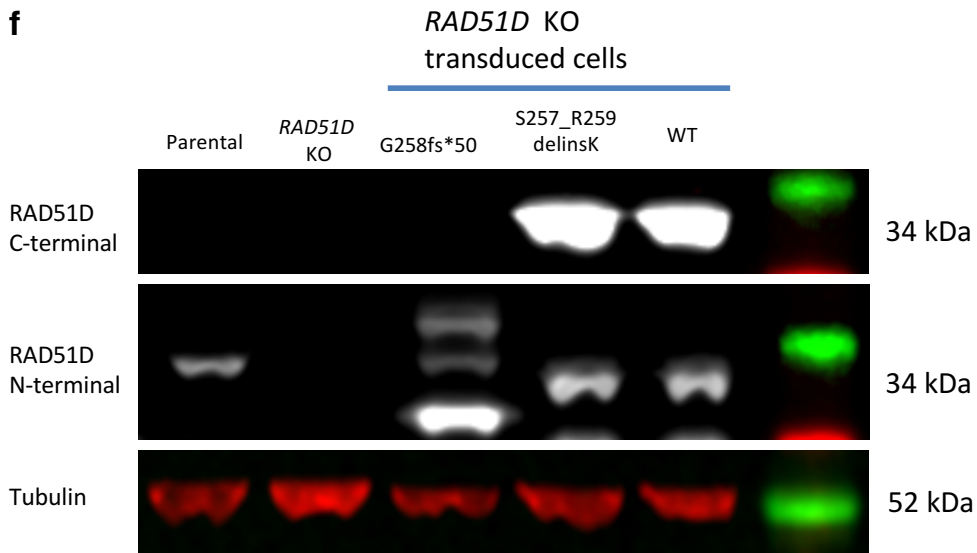
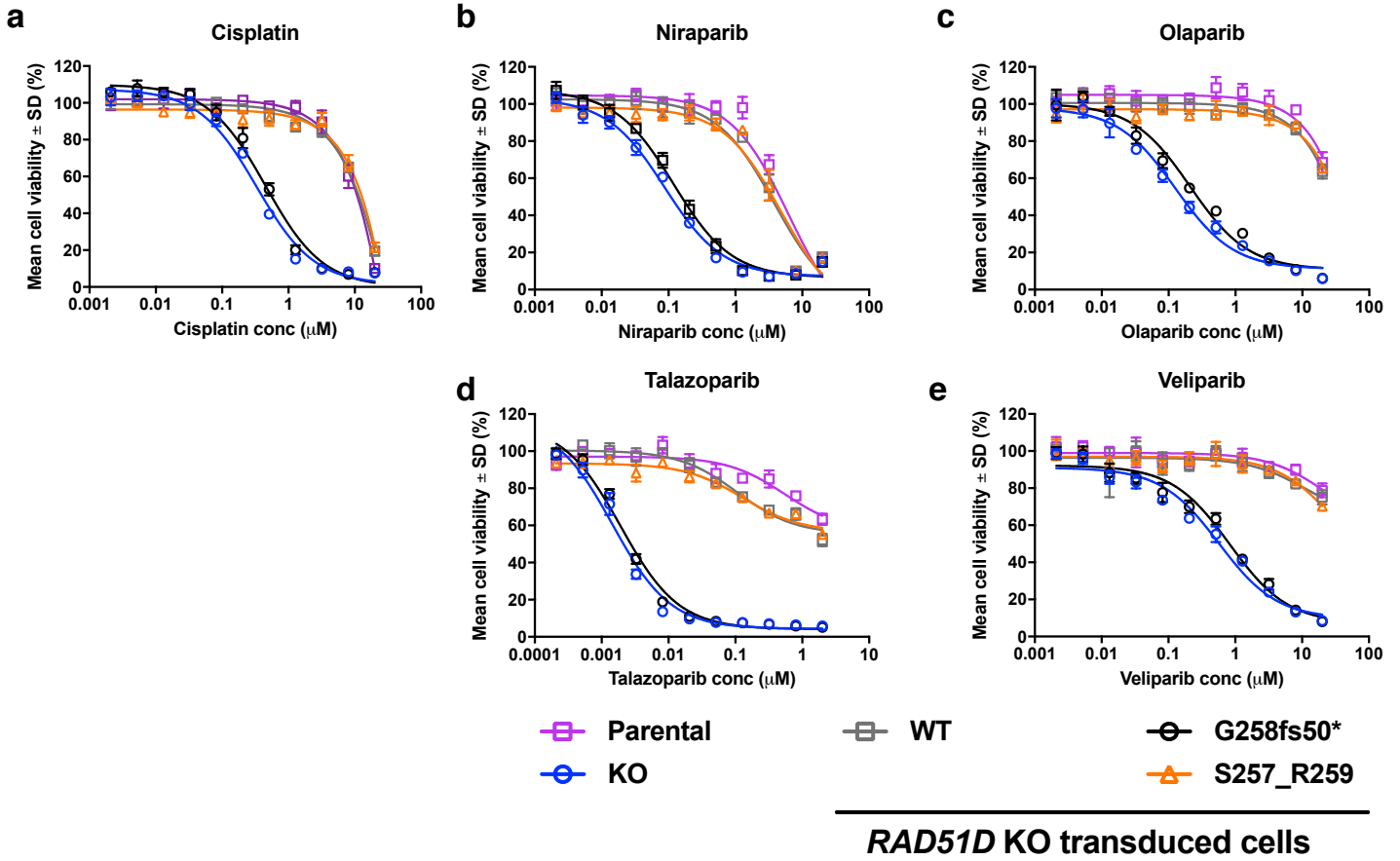


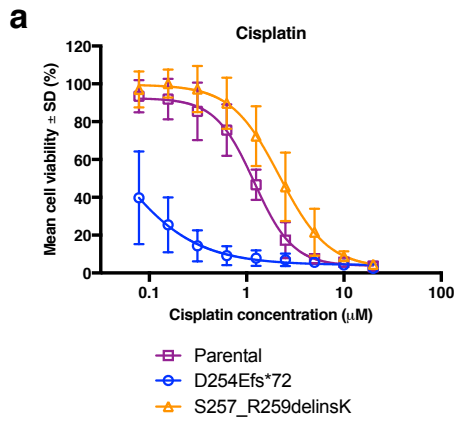
	R193*	R193R	HR192_193GG	WT (normal tissue)
Section I	66.00%	30.00%	0.13%	3.86%
Section II	65.87%	27.56%	0.27%	6.30%
Section III	64.18%	27.84%	0.17%	7.74%
Section IV	65.60%	26.66%	0.15%	7.49%
Section V	62.43%	24.01%	0.45%	13.01%
Section VI	63.69%	22.27%	0.70%	13.28%



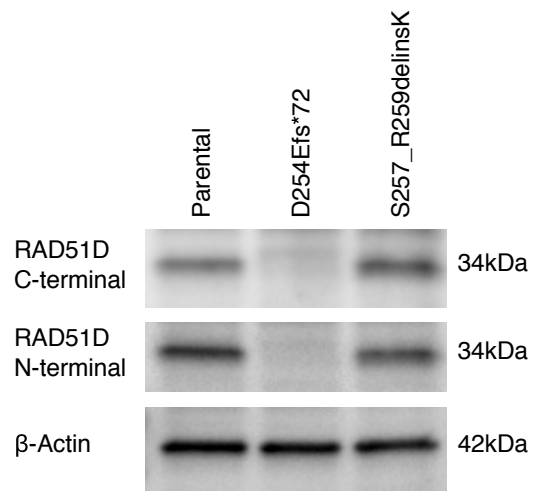
d

	222	555	789	
Human	VTN	HITRDRD	SGRLK	PALGRSWSFVPSTRILLDT-IE
Gorilla	VTN	HITRDRD	SGRLK	PALGRSWSFVPSTRILLDT-IE
Chimp	VTN	HITRDRD	SGRLK	PALGRSWSFVPSTRILLDT-IE
Orangutan	VTN	HITRDRD	SRRLK	PALGRSWSFVPSTRILLDT-IE
Gibbon	VTN	HITRDRD	SGRLK	PALGRSWSFVPRTRILLDT-IE
Vervet	VTN	HITRDRD	SGRLK	PALGRSWSFVPSTRILLDA-IE
Olive baboon	VTN	HITRDRD	SGRLK	PALGRSWSFVPSTRILLDT-IE
Marmoset	VTN	HITRDRD	SGRLK	PALGHSWSFVPSTRILLDT-IN
Tarsier	VTN	HITRDRD	SGRLK	PALGRSWSFVPSTRILLNV-IE
Bushbaby	VTN	HITRDRD	SGRLK	PALGRSWSFVPSTRIFLDI-IE
Mouse	VTN	HLTRDWD	GRRFK	PALGRSWSFVPSTRILLDV-TE
Rat	VTN	HLTRDRD	SRRFK	PALGRSWSFVPSTRILLEV-FE
C.Hamster	VTN	HLTRDRD	GRRFK	PALGRSWSFVPSTRILLDV-TK
Squirrel	VTN	HITRDRD	SGKFK	PALGRSWSFVPSTRILLDI-IE
Guinea Pig	VTN	HITRDRD	SGRLK	PALGRSWSFVPSTRVLLDS-IE
Pika	VTN	HITQDRE	SGKVK	PALGRSWSFVPNTRVLLGI-PE
Sheep	VTN	HITRDRD	SGQLK	PALGRSWSFVPSTRLLLDS-TQ
Cow	VTN	HITRDRD	SGQLK	PALGRSWSFVPSTRLLLDS-TQ
Pig	VTN	HITRDRD	SGKHK	PALGRSWSFVPSTRLLLDI-SQ
Dolphin	VTN	HITRDRD	SGQLK	PALGRSWSFVPSTRLLLDI-GQ
Dog	VTN	HITRDRD	SGELK	PALGRSWSFVPSTRILLDI-DE
Panda	VTN	HITRDRD	SGDLK	PALGRSWSFVPSTRILLDV-DK
Cat	VTN	HITRDRD	SGKLL	PALGRSWSFVPSTRILLDI-EE
Horse	VTN	HITRDRD	SGKLL	PALGRSWSFVPSTRILLDT-GE
Microbat	VTN	HITRDRD	SGKLL	PALGRSWSFVPSTRVILAI-GE
Megabat	VTN	HITRDRD	SGKFK	PALGRSWSFVPSTRIVLAI-GE
Shrew	VTN	HLTRDRD	SGRLK	PALGRAWFVPNTRILLDVGGGE
Hedgehog	VTN	HITRDRD	SGKLL	PALGLSWSFVPSTRILLDL-GE
Tenrec	VTN	QVTRERD	SGKLR	PALGRSWSFVPNTRVLLDV-DE
Hyrax	VTN	HITRDRD	SGRVR	PALGRSWSFVPSTRILLDV-SE
Elephant	VTN	HITRDRD	SGRLK	PALGRSWSFVPSTRILLAV-GE
Armadillo	VTN	HITRDRD	SGKIK	PALGRSWSFVPSTRVLLGV-GE
Opossum	VTN	HITRDRD	SGVLK	PALGRSWSFVPSTRVLLVLEA-RE
TasmanianDevil	VTN	HITREWENG	KLR	PALGRSWSFVPSTRVLLVLEA-WE





b



Foundation Medicine sequencing of RAD51C mutant post-progression biopsy

	Amino acid	DNA	Number of reads	Allele frequency
WT(ref genome)	HR	CACCGA	128	14.6%
Initial germline mutation	H*	CACTGA	555	63.2%
Resistance mutation 1	HW	CACTGG	90	10.3%
Resistance mutation 2	HR	CACAGA	60	6.8%
Resistance mutation 3	GG	GGCGGA	25	2.9%
Resistance mutation 4	HL	CACTTA	20	2.3%

Proposed model of sample that is compatible with observed allele frequency and copy number model

